Title

Apamin does not inhibit human cardiac Na+ current, L-type Ca2+ current or other major K+ currents.

Journal

PLoS ONE, 9(5)

Authors

Yu, Chih-Chieh
Ai, Tomohiko
Weiss, James
et al.

Publication Date

2014

DOI

10.1371/journal.pone.0096691

Peer reviewed

OPEN ACCESS Freely available online

PLOS ONE

Apamin Does Not Inhibit Human Cardiac Na^+ Current, L-type Ca^{2+} Current or Other Major K^+ Currents

Chih-Chieh Yu[1,2], Tomohiko Ai[1,3], James N. Weiss[4], Peng-Sheng Chen[1]*

1 Krannert Institute of Cardiology and Division of Cardiology, Department of Medicine, Indiana University School of Medicine, Indianapolis, Indiana, United States of America, **2** Department of Integrated Diagnostic & Therapeutics, National Taiwan University, Taipei, Taiwan, **3** Department of Molecular Pathogenesis, Division of Pathophysiology, Medical Research Institute, Tokyo Medical and Dental University, Tokyo, Japan, **4** Cardiovascular Research Laboratory, Departments of Medicine (Cardiology) and Physiology, David Geffen School of Medicine, University of California Los Angeles, Los Angeles, California, United States of America

Abstract

Background: Apamin is commonly used as a small-conductance Ca^{2+}-activated K^+ (SK) current inhibitor. However, the specificity of apamin in cardiac tissues remains unclear.

Objective: To test the hypothesis that apamin does not inhibit any major cardiac ion currents.

Methods: We studied human embryonic kidney (HEK) 293 cells that expressed human voltage-gated Na^+, K^+ and Ca^{2+} currents and isolated rabbit ventricular myocytes. Whole-cell patch clamp techniques were used to determine ionic current densities before and after apamin administration.

Results: Ca^{2+} currents (CACNA1c+CACNB2b) were not affected by apamin (500 nM) (data are presented as median [25th percentile;75th percentile] (from −16 [−20;−10] to −17 [−19;−13] pA/pF, P = NS), but were reduced by nifedipine to −1.6 [−3.2;−1.3] pA/pF (p = 0.008). Na^+ currents (SCN5A) were not affected by apamin (from −261 [−282;−145] to −268 [−379;−132] pA/pF, P = NS), but were reduced by flecainide to −57 [−70;−47] pA/pF (p = 0.018). None of the major K^+ currents (I_{Ks}, I_{Kr}, I_{K1} and I_{to}) were inhibited by 500 nM of apamin (KCNQ1+KCNE1, from 28 [20;37] to 23 [18;32] pA/pF; KCNH2+KCNE2, from 28 [24;30] to 27 [24;29] pA/pF; KCNJ2, from −46 [−48;−40] to −46 [−51;−35] pA/pF; KCND3, from 608 [505;748] to 606 [454;684]). Apamin did not inhibit the I_{Na} or I_{CaL} in isolated rabbit ventricular myocytes ($I_{Na,}$ from −67 [−75;−59] to −68 [−71;−59] pA/pF; I_{CaL}, from −16 [−17;−14] to −14 [−15;−13] pA/pF, P = NS for both).

Conclusions: Apamin does not inhibit human cardiac Na^+ currents, L-type Ca^{2+} currents or other major K^+ currents. These findings indicate that apamin is a specific SK current inhibitor in hearts as well as in other organs.

Citation: Yu C-C, Ai T, Weiss JN, Chen P-S (2014) Apamin Does Not Inhibit Human Cardiac Na^+ Current, L-type Ca^{2+} Current or Other Major K^+ Currents. PLoS ONE 9(5): e96691. doi:10.1371/journal.pone.0096691

Editor: Steven Barnes, Dalhousie University, Canada

Received January 14, 2014; **Accepted** April 10, 2014; **Published** May 5, 2014

Funding: Research reported in this manuscript was supported by the National Heart, Lung and Blood Institute of the National Institutes of Health under award number P01HL78931, R01HL71140, a Medtronic-Zipes Endowment (P.-S.C.) and the Indiana University Health-Indiana University School of Medicine Strategic Research Initiative. The funders had no role in study design, data collection and analysis, decision to publish, or preparation of the manuscript.

Competing Interests: The authors have declared that no competing interests exist.

* E-mail: chenpp@iu.edu

Introduction

Small-conductance calcium activated potassium (SK) channels, which are abundantly present in the central nervous system [1], were first cloned in 1996 by Kohler *et al* [2]. Study of this channel is facilitated by the use of apamin, which has been thought to be a specific inhibitor of SK current in the nervous system [1,3,4]. Subsequent investigations showed that the apamin-sensitive potassium current (I_{KAS}) is present in the atria [5–12]. In addition, while normal ventricles paced at physiological cycle lengths do not express significant I_{KAS} [13], we and others found that I_{KAS} expression is upregulated in failing, ischemic or infarcted human, rabbit and rat ventricles and in normal rabbit ventricles with complete atrioventricular block [14–19]. A common criticism of all these studies is that the specificity of apamin in cardiac type ion channels has not been well established. Some previous studies have shown that apamin inhibits fetal L-type Ca^{2+} currents [20–22] and Na^+ currents [23] in the chick heart, suggesting that apamin may have off target effects on other cardiac ion channels. However, there is no information on the effects of apamin on Na^+, Ca^{2+} and K^+ currents that are responsible for adult human cardiac activation and repolarization. Because I_{KAS} is potentially important in human cardiac arrhythmogenesis, it is important to establish whether apamin is a specific SK current inhibitor as apamin is used to define I_{KAS}. The purpose of the present study was to test the hypothesis that apamin is a specific inhibitor of I_{KAS} in adult human cardiac ion channels. We tested that hypothesis by performing patch clamp studies of major cardiac ion channels expressed in human embryonic kidney (HEK) 293 cells and by testing the effects of apamin on Na^+ and Ca^{2+} currents in rabbit ventricular myocytes.

Materials and Methods

The study was approved by the Institutional Biosafety Committee and Institutional Animal Care and Use Committee of the Indiana University and the Methodist Research Institute, Indianapolis, Indiana.

Cell Culture and Gene Transfection

Human embryonic kidney (HEK) 293 cells were cultured in Iscove's Modified Dulbecco's Medium (Gibco) with 10% fetal bovine serum and 1% penicillin/streptomycin in 5% CO_2 at 37°C. To study human Nav1.5, a stable HEK 293 cell line expressing consistent sodium currents (I_{Na}) was used [24]. Other than I_{Na}, 35 mm dishes of HEK 293 cells were transiently transfected using Effectene Transfection Reagent (Qiagen) according to the manufacturer's protocol and were harvested for patch clamp experiment 48~72 hours later. The amount and content of plasmids transfected for each channel were described as followings: for I_{Ca}, 1.5 μg of CACNA1c/pcDNA3.1 and 2.0 μg of CACNB2b/pIRES2-DsRed-Express were co-transfected; for I_{Ks}, 1 μg of KCNQ1/pIRES2-EGFP and 1 μg of KCNE1/pIRES-CD8 were co-transfected; for I_{Kr}. 3 μg of KCNH2/pIRES-hyg and 1 μg of KCNE2/pIRES2-DsRed-Express were co-transfected; for I_{K1}, 2 μg of KCNJ2/pCMS-EGFP were transfected; and for I_{to}, 2 μg of KCND3/pIRES2-DsRed-Express were transfected.

The stably SK2-expressing cells were used for positive control studies to test the effects of apamin. The SK2 clone was developed in our laboratory. HEK 293 cells were transfected with 2.0 μg of KCNN2/pIRES-hyg plasmids. Single cells were picked and propagated in selection media containing hygromycin 200 μg/ml. Expression of I_{SK2} was verified by patch-clamp measurements.

Rabbit Cardiomyocyte Isolation

The rabbits were intravenously injected with 1,000 units of heparin and anesthetized with sodium pentobarbital (100 mg/kg). After a median sternotomy, the hearts were rapidly excised, mounted onto a Langendorff perfusion apparatus and perfused for 4 minutes with 37°C oxygenated Ca^{2+}-free buffer. The composition of the buffer was (in mM) NaCl 136, KCl 5.4, NaH_2PO_4 0.33, $MgCl_2$ 1.0, HEPES 10 and glucose 10, adjusted to pH 7.4 with NaOH. After the blood was washed out, the heart was recirculated with enzyme solution, containing 1 mg/ml collagenase type II (Worthington, Lakewood, NJ) and 0.1 mg/ml protease (Sigma-Aldrich, St. Louis, MO, USA) in the same buffer for 28 minutes, followed by another 4 minutes of washing with Ca^{2+}-free buffer. The heart was then removed from the apparatus and the ventricle was triturated. The isolated cardiomyocytes were washed and titrated up with Ca^{2+}-containing Tyrode's solution until the Ca^{2+} level reaches 1.8 mM.

Patch-clamp Experiments

Whole cell configuration of the voltage-clamp technique was used in this study as described elsewhere [25]. Briefly, whole-cell configuration was made in Tyrode's solution. Pipette resistances were 1.5–3 MΩ. After achieving a gigaseal, the test-pulse current was nulled by adjusting the pipette capacitance compensator with both fast and slow components. After break-in, the whole-cell charging transient was nulled by adjusting whole cell capacitance and series resistance. Voltage control protocols were generated with Axopatch 200B amplifier/Digidata 1440A acquisition system using pCLAMP-10 software (Molecular Devices/Axon, Sunnyvale, CA). Whole-cell recording was analyzed using Clampfit 10.2. To measure I_{SK2}, we used Tyrode's solution as the bath solution containing (in mM) NaCl 140, KCl 5.4, $MgCl_2$ 1.2, HEPES 5, NaH_2PO_4 0.33, $CaCl_2$ 1.8 and Glucose 10 (pH 7.4 adjusted with NaOH). The pipette solution contained (in mM) K-Gluconate 144, $MgCl_2$ 1.15, EGTA 1, HEPES 10 and free Ca^{2+}1 μM (pH 7.2 adjusted with KOH). All experiments for I_{SK2} were carried out at 37°C. For measuring I_{Na}, we used Tyrode's solution (see above) as the bath solution. The pipette solution contained (in mM) NaF 10, CsF 110, CsCl 20, EGTA 10, and HEPES 10 (pH 7.35 adjusted with CsOH). After testing apamin 500 nM, fleicainide 100 μM was used as a positive control [26]. For measuring I_{Ca}, we replaced extracellular calcium with barium to lessen the rundown phenomenon [27,28]. The bath solution contained (in mM) $BaCl_2$ 5, NaCl 130, $MgCl_2$ 1.0, HEPES 10, and Glucose 11 (pH 7.4 adjusted with NaOH). The pipette solution contained (in mM) CsCl 120, $MgCl_2$ 2, EGTA 10, HEPES 10, Mg-ATP 5, Na_2-GTP 1.5 and cAMP 1 (pH 7.24 adjusted with CsOH). Nifedipine 2 μM was used as the positive control [29]. All experiments for I_{Ba} were carried out at 37°C. For measuring I_{Ks}, we used Tyrode's solution as the bath solution (see above). The pipette solution contained (in mM) KCl 130, KOH 20, EGTA 5, Mg-ATP 5, HEPES 5, cAMP 0.05 and Na_2-GTP 0.1 (pH 7.4 adjusted with KOH). Chromanol 293B 50 μM was used as the positive control [30]. For measuring I_{Kr}, I_{K1} and I_{to}, we used Tyrode's solution (see above) as the bath solution. The pipette solution contained (in mM) KCl 130, KOH 20, EGTA 5, Mg-ATP 5 and HEPES 5 (pH 7.4 adjusted with KOH). E4031 100 nM, CsCl 5 mM and 4-aminopyridine 10 mM were used as the positive control, respectively [31–33]. To measure I_{Na} and I_{Ca} in rabbit cardiomyocytes, we used Tyrode's solution as the bath solution (see above), and the pipette solution contained (in mM) aspartate 85, TEACl 20, $MgCl_2$ 2, EGTA 10, HEPES 10, Mg-ATP 5, and Na_2-GTP 5 (pH 7.2 adjusted with KOH).

Stable current density during baseline solution superperfusion was measured immediately before the addition of apamin to define baseline current density. This was followed by superfusion with 500 nM apamin for at least 3 minutes until the current became stable. Following apamin exposure, specific blockers of each current were used as positive controls.

Drugs and Reagents

Apamin (catalog#1652), was purchased from Tocris Bioscience (Minneapolis, MN) and was dissolved in water for a 250 μM stock solution. Apamin was freshly diluted with bath solution daily before experiment. Flecainide (catalog#1470), chromanol 293B (catalog#1412) and E4031 (catalog#1808) were purchased from Tocris. All other chemicals were purchased from Sigma-Aldrich (St. Louis, MO).

Statistical Analysis

Summary data following apamin or positive controls were normalized to baseline. Nonparametric tests were used in this whole experiment. Related-samples Friedman's Two-Way Analysis of Variance by Ranks was conducted to compare continuous variables among baseline, post apamin and post specific blockers. Related-Samples Wilcoxon Signed Rank Test was performed for post-hoc analysis. I_{Ks} rundown was quantified by the time constant (τ) of a single exponential fit of the current. Independent-samples Mann-Whitney U test was performed to compare τ of rundown with and without apamin. P value less than 0.05 was considered statistically significant. Statistical analyses were performed using SPSS (IBM, Chicago, IL, USA, version 21). Data in text and figures are presented as median [25^{th} percentile;75^{th} percentile].

Results

Studies in HEK 293 Cells

Apamin's effects on I_{SK2}. Figure 1 shows that untransfected HEK 293 cells expressed very low levels of endogenous potassium currents (<100 pA) compared to the nA levels of currents observed after transfection with various ion channels (see figure legends and subsequent figures). Figure 2A and 2B show the representative tracings and time course of I_{SK2} in transfected HEK 293 cells, induced by a repetitive voltage-ramp pulses (from +40 to –100 mV, 400 ms duration) from a holding potential of –50 mV. A total 8 cells were tested at 37°C. The currents became stable 4~8 minutes after the whole-cell configuration was made. Subsequent application of apamin (500 nM) reduced the currents by 99±4%. Figure 2C shows the summary data before and after apamin.

Apamin does not inhibit I_{Na}. Figures 3A and 3B show the representative tracings and time course of I_{Na} at a frequency of 20/min. The I_{Na} was induced by a repetitive depolarization pulse (to –10 mV for 300 ms) from a holding potential of –140 mV. All experiments were carried out in room temperature. A total of 9 cells were tested and no significant inhibition or enhancement was observed after adding 500 nM apamin. The median baseline current density was –261 [–282;–145] pA/pF. The averaged current density after apamin was –268 [–379;–132] pA/pF (n = 9, p = 0.767, compared to the baseline). The averaged current density after flecainide was –57 [–70;–47] pA/pF (n = 7; p = 0.018 compared to post apamin, p = 0.018 compared to baseline). Figure 3C shows the summary of drug effects normalized to the baseline.

Apamin does not inhibit I_{Ba}. Figures 3D and 3E show the representative tracings and time course of I_{Ba} in the presence of apamin 500 nM or nifedipine 2 μM. I_{Ba} was induced by a step pulse protocol (to 0 mV for 500 ms) from a holding potential of –80 mV and a brief prepulse at –40 mV. A total of 8 cells were tested. No significant effects of apamin were observed on I_{Ba}. The baseline current density of I_{Ba} was –16 [–20;–10] pA/pF. The current density after apamin was 17 [–19;–13] (n = 8, p = 0.953, compared to baseline), and –1.6 [–3.2;–1.3] pA/pF after nifedipine (n = 8; p = 0.008 compared to post apamin, p = 0.008 compared to baseline). I_{Ca} had also been studied using 1.8 mM Ca^{2+} in the external solution. However, it was difficult to study the effects of apamin on I_{Ca} due to a marked rundown phenomenon. Apamin did not show significant effects during rundown (Figure S1).

Apamin does not inhibit I_{Ks}. A rundown phenomenon was also observed in the study of I_{Ks} (Figure 4A). Various concentrations of apamin (from 0.5 fM to 500 nM) were applied during rundown, but the time course of rundown was not affected (Figure 4B). Figure 4C summarizes the time constant (τ) of rundown with and without apamin. There were no significant differences between the two. Figures 5A and 5B show the representative tracings and time course of I_{Ks}. I_{Ks} was induced with a 4s depolarization pulse protocol (to +40 mV) from a holding potential of –80 mV. The baseline current density of I_{Ks} was 28 [20;37] pA/pF. After apamin, the average current density was 23 [18;32] pA/pF (n = 10, p = 0.037, compared to the baseline). After adding 50 μM Chromanol 293B, the current density was reduced to 4.7 [4.1;6.7] pA/pF (n = 6; p = 0.028 compared to post apamin, p = 0.028 compared to baseline). Figure 5C shows the summary of drug effects normalized to baseline.

Apamin does not inhibit I_{Kr}. Figures 5D and 5E represent tracings and the time course of apamin effect on I_{Kr}. The current was induced by a depolarization pulse (to +20 mV for 4 s in duration) from a holding potential of –80 mV, and measured as the peak tail current at –50 mV, repeated every 10 s. Apamin had no significant effect. The baseline current density of I_{Kr} was 28 [24;30] pA/pF, and was 27 [24;29] pA/pF after apamin (n = 6, p = 0.345, compared to baseline). The current density was reduced

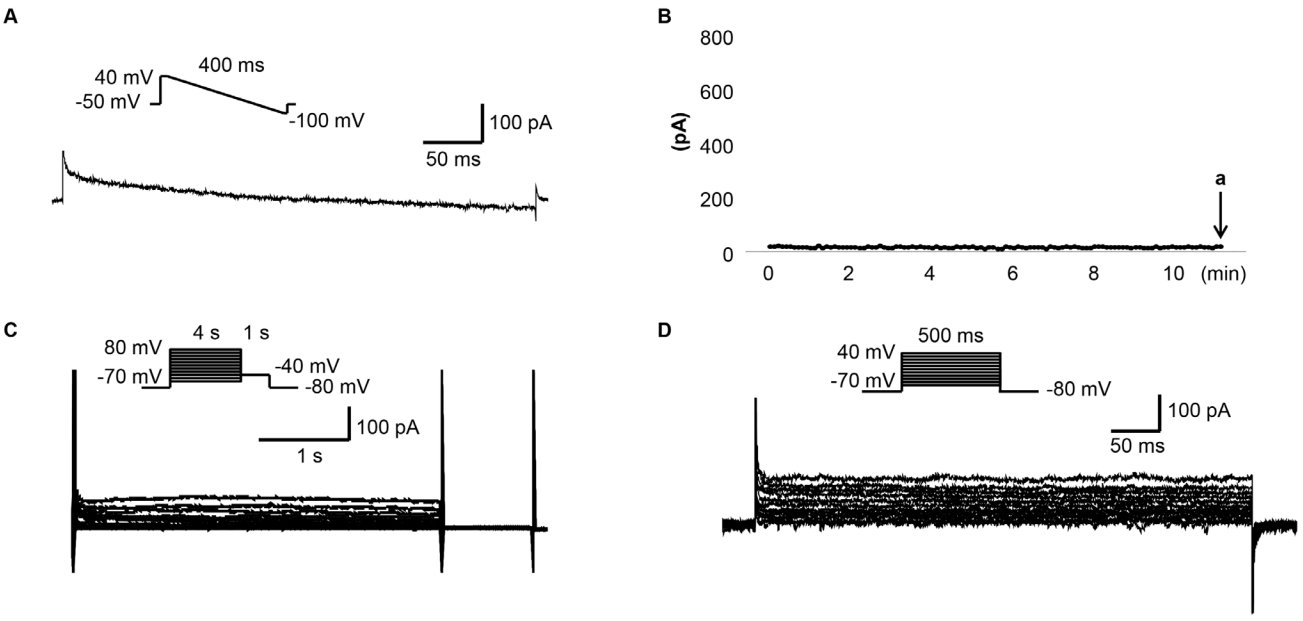

Figure 1. The endogenous K^+ currents of HEK 293 cells. (A) The representative tracing obtained with ramp protocol shown in the inset at time point indicated by arrow a in (B). The pipette and bath solutions are the same as the ones used in measuring I_{SK2}. (B) The time course of I_{SK2} measured at 0 mV. (C) The representative tracings obtained with the pulse protocol shown in the inset with the pipette and bath solution used in measuring I_{Ks}. (D) The representative tracings obtained with the pulse protocol shown in the inset with the pipette and bath solutions used in measuring I_{Kr}, I_{K1} and I_{to}.

doi:10.1371/journal.pone.0096691.g001

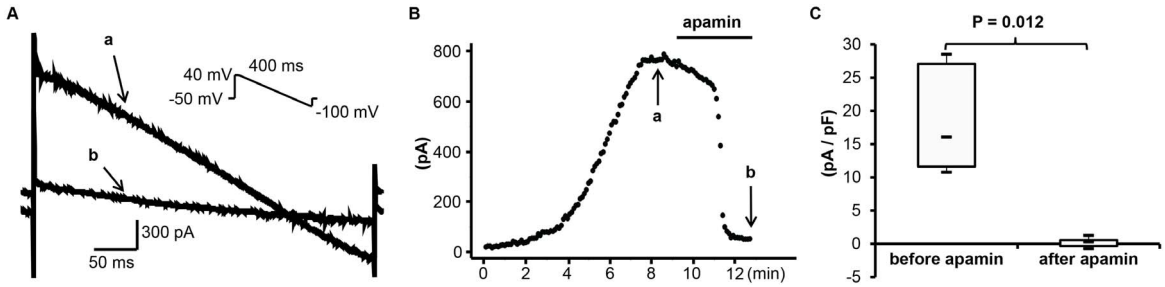

Figure 2. Effect of apamin on I_{SK2} in transfected HEK 293 cells. (A) The representative I_{SK2} tracings obtained by the descending voltage ramp protocol shown in the inset before (a) and after (b) apamin at time points indicated by arrows a and b in (B). (B) The time course of I_{SK2} at 0 mV. (C) The summary of current density before and after apamin.
doi:10.1371/journal.pone.0096691.g002

to 10 [8;14] pA/pF by E4031 (n = 5; p = 0.043 compared to post apamin, p = 0.043 compared to baseline). Figure 5F shows the summary of drug effects normalized to baseline.

Apamin does not inhibit I_{K1}. Figures 6A and 6B show the representative time course and tracings of I_{K1} in the absence and presence of apamin (500 nM). The I_{K1} was induced by a ramp pulse protocol between –120 mV and 40 mV (1 s in duration, every 5 s) from a holding potential of –80 mV. The current at –100 mV was monitored and shown in Figure 4B. No significant effects were observed after adding apamin. The baseline current density of I_{K1} was –46 [–48;–40] pA/pF. After apamin administration, the average current density was –46 [–51;–35] pA/pF (n = 7, p = 0.612, compared to baseline). CsCl reduced the current density to –18 [–27;–15] pA/pF (n = 7; p = 0.018 compared to post apamin, p = 0.018 compared to baseline). Figure 6C shows the summary of drug effects normalized to baseline.

Apamin does not inhibit I_{to}. Figures 6D and 6E show the effect of apamin on I_{to}. The current was induced by a repetitive depolarization pulse (+20 mV for 500 ms in duration) from a holding potential of –80 mV. Apamin had no significant effect. The baseline current density of I_{to} was 608 [505;748] pA/pF, and was 606 [454;684] pA/pF after apamin (n = 13, p = 0.052, compared to baseline). The current density was reduced to 247 [228;323] pA/pF by 4-aminopyridine (n = 12; p = 0.001 compared to apamin's effect, p = 0.002 compared to baseline). Figure 6F shows the summary of drug effects normalized to baseline.

Studies in Rabbit Cardiomyocytes

Apamin does not inhibit the native I_{Ca}. Figures 7A and 7B show the representative tracings and time course of I_{Ca} in the presence of apamin 500 nM or nifedipine 2 μM. I_{Ca} was induced by a step pulse protocol (to 0 mV for 500 ms) after a brief prepulse to –40 mV from a holding potential of –80 mV to inactivate I_{Na}.

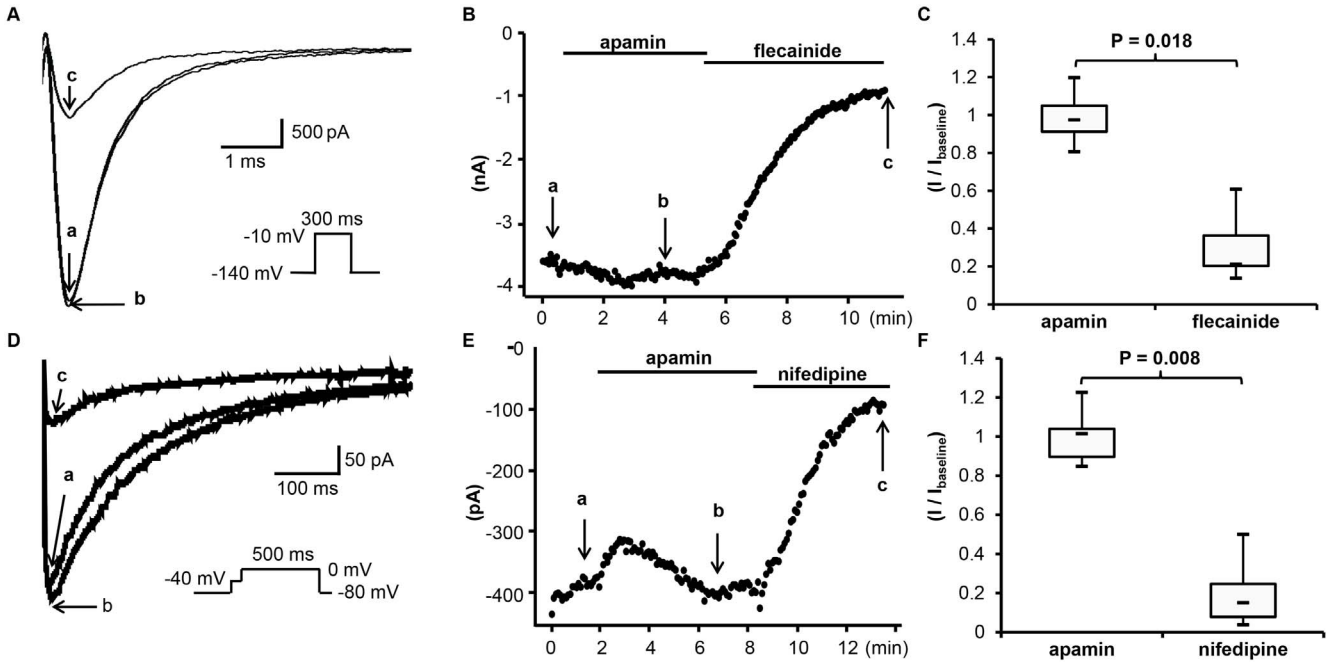

Figure 3. Effects of apamin on I_{Na} and I_{Ba} in transfected HEK 293 cells. (A) The representative I_{Na} tracings obtained by the pulse protocol shown in the inset before apamin (a), after apamin (b) and after flecainide (c) at time points indicated by arrows a through c, respectively, in (B). (B) The time course of peak I_{Na} measured at –10 mV. (C) The summary of drug effects normalized to baseline. (D) The representative I_{Ba} tracings at 0 mV obtained by the pulse protocol shown in the inset before apamin (a), after apamin (b) and after nifedipine (c) at time points indicated by arrows a through c, respectively, in (E). (E) The time course of peak I_{Ba} measured at 0 mV. (F) The summary of drug effects normalized to baseline.
doi:10.1371/journal.pone.0096691.g003

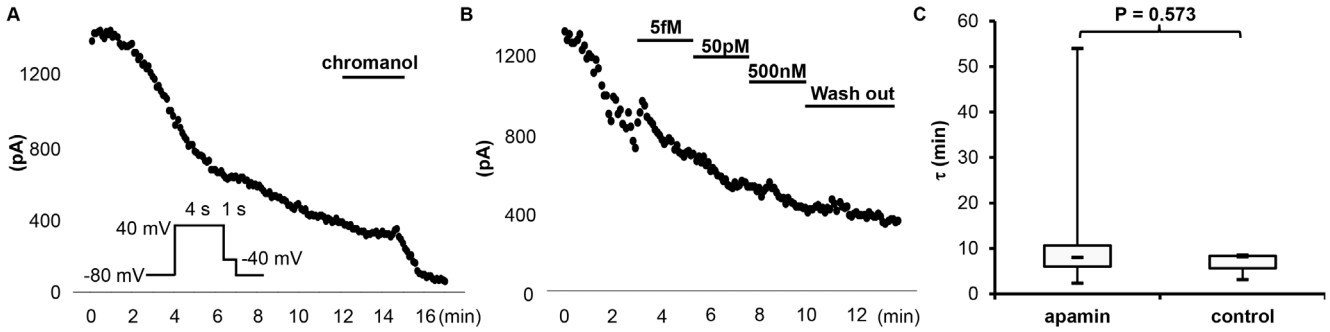

Figure 4. Effects of different concentrations of apamin on the rundown course of I_{Ks} in transfected HEK 293 cells. (A) An observation experiment without apamin treatment showing time-dependent rundown, obtained with the pulse protocol shown in the inset with chromanol 293B at the end. (B) The representative time course of I_{Ks} treated with different concentrations of apamin. (C) The time constant (τ) of the rundown curve with (n = 10) and without (n = 3) apamin.
doi:10.1371/journal.pone.0096691.g004

Apamin had no significant effects on I_{Ca}. The current density of I_{Ca} averaged –16 [–17;–14] pA/pF at baseline, and –14 [–15;–13] pA/pF after apamin (n = 7, p = 0.091, compared to the baseline). After adding 2 μM of nifedipine, the current density was reduced to –3.9 [–5.8;–2.6] pA/pF (n = 7; p = 0.018 compared to post apamin, p = 0.018 compared to baseline). Figure 7C shows the summary of drug effects normalized to baseline.

Apamin does not inhibit the native I_{Na}. In the same experiments, the native cardiac I_{Na} was also measured during the prepulse to –40 mV. Figure 7D and 7E showed the representative tracings and time course of I_{Na} before and after apamin. There was no significant change after adding apamin. The baseline current density of I_{Na} was –67 [–75;–59] pA/pF, and was –68 [–71;–59] pA/pF after apamin (n = 6; p = 0.753 compared to the baseline). Figure 7F shows the summary of drug effects.

Discussion

We found that at a concentration of 500 nM, apamin has no significant effects on major cardiac ion currents that underlie the action potential in human hearts, including L-type Ca^{2+}, Na^+ and the major K^+ currents (I_{Ks}, I_{Kr}, I_{K1}, I_{to}). This finding suggests that apamin at this concentration can be used to study the role of SK currents in human cardiomyocytes.

Apamin as a specific ion channel inhibitor. Apamin is a peptide toxin isolated from Western honey bees [34]. When injected with 0.5 mg/kg or more of apamin, mice develop neurological symptoms including spasms, jerks and convulsions of apparently spinal origin [34]. Subsequent studies showed that apamin is a highly selective SK channel inhibitor in the central nervous system. Because SK channels are the only known targets

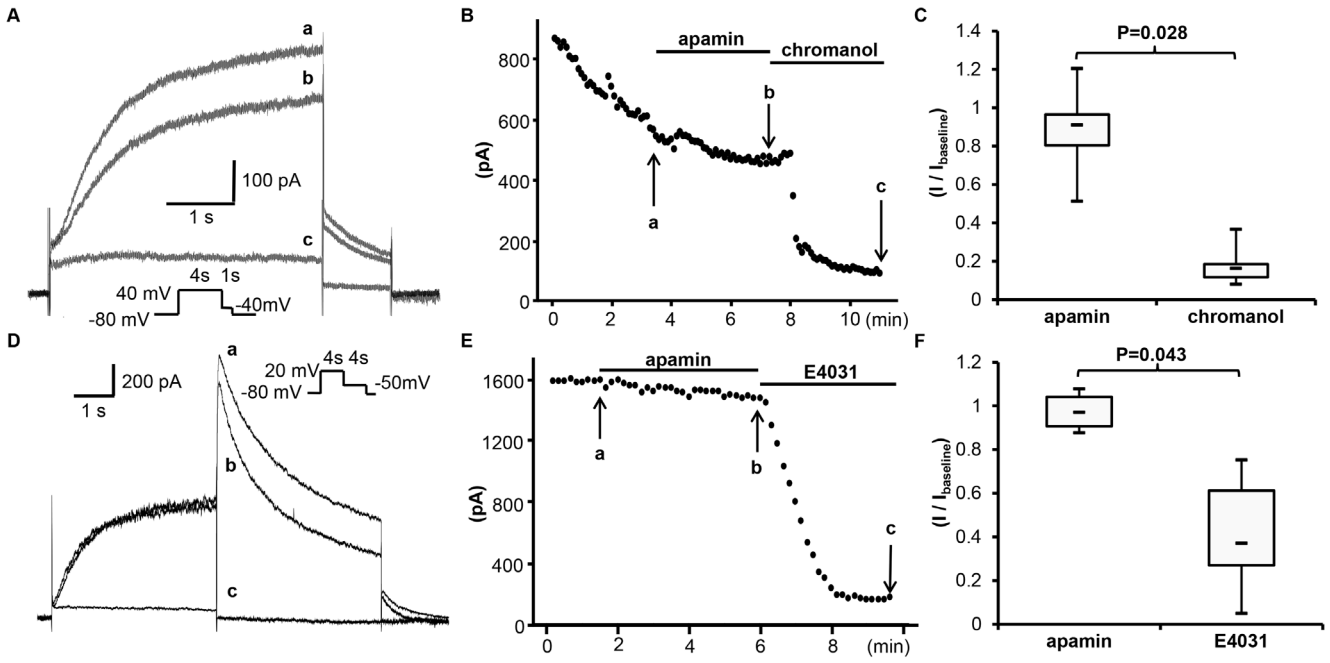

Figure 5. Effects of apamin on I_{Ks} and I_{Kr} in transfected HEK 293 cells. (A) The representative tracings of I_{Ks} obtained by pulse protocol shown in the inset before apamin (a), after apamin (b) and after chromanol (c) at time points indicated by arrows a through c, respectively, in (B). (B) The time course of peak I_{Ks} at 40 mV. (C) The summary of drug effects normalized to baseline. (D) The representative tracings of I_{Kr} obtained by a pulse protocol shown in the inset before apamin (a), after apamin (b) and after E4031 (c) at time points indicated by arrows a through c in (E). (E) The time course of peak I_{Kr} at 20 mV. (F) The summary of drug effects normalized to baseline.
doi:10.1371/journal.pone.0096691.g005

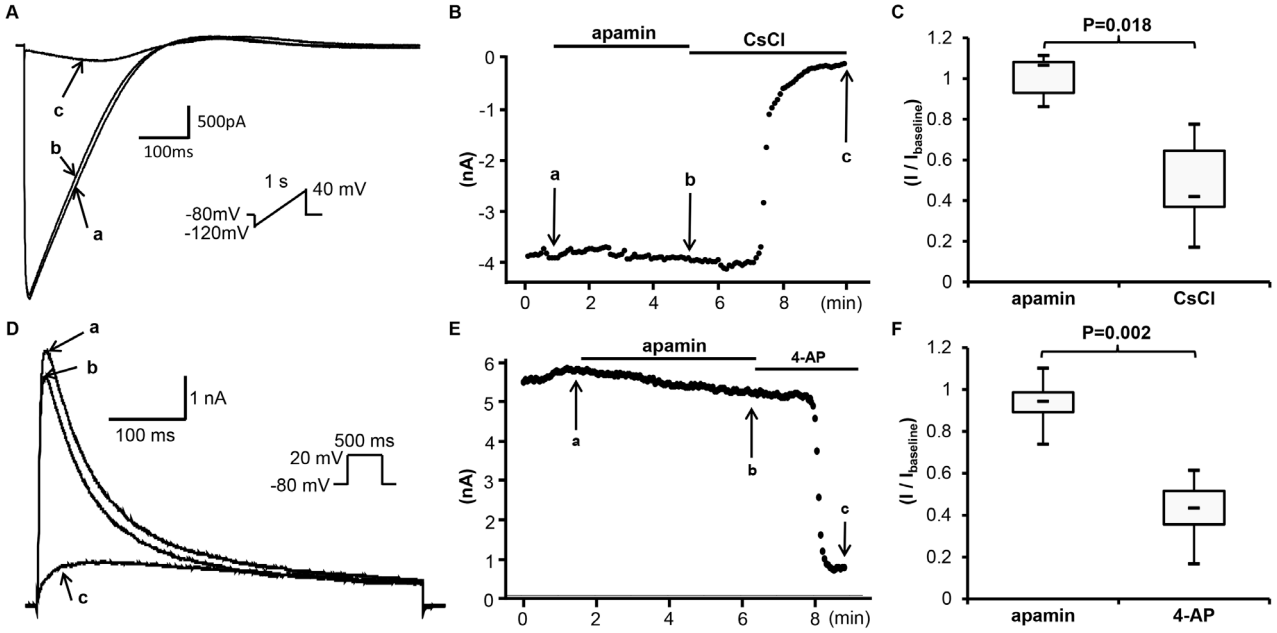

Figure 6. Effects of apamin on I_{K1} and I_{to} in transfected HEK 293 cells. (A) The representative tracings of I_{K1} by ascending voltage ramp protocol shown in the inset before apamin (a), after apamin (b) and after CsCl (c) at time points indicated by arrows a through c, respectively, in (B). (B) The time course of I_{K1} at −100 mV. (C) The summary of drug effects normalized to baseline. (D) The representative tracings of I_{to} obtained by a pulse protocol shown in the inset before apamin (a), after apamin (b) and after 4-AP (c) at time points indicated by arrows a through c, respectively, in (E). (E) The time course of peak I_{to} at 20 mV. (F) The summary of drug effects normalized to baseline.
doi:10.1371/journal.pone.0096691.g006

for apamin, the effects of apamin at the molecular, cellular, and behavioral levels may be ascribed to SK channel blockade [35]. The specificity of apamin in the central nervous system has contributed significantly to the understanding of SK channel function in controlling activation and repolarization of neurons. Since 2003, apamin-sensitive K currents have also been known to

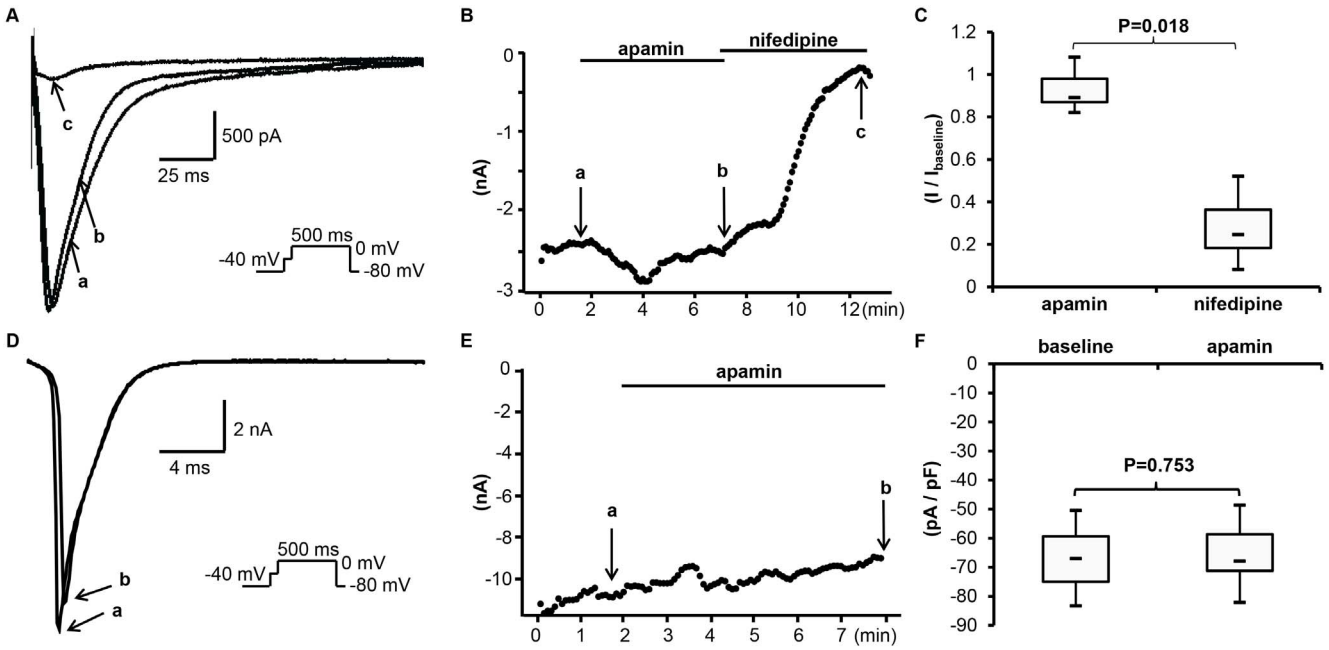

Figure 7. Effects of apamin on I_{Ca} and I_{Na} in rabbit cardiomyocytes. (A) The representative I_{Ca} tracings obtained by a pulse protocol shown in the inset before apamin (a), after apamin (b) and after nifedipine (c) at time points indicated by arrows a through c, respectively, in (B). (B) The time course of peak I_{Ca} measured at 0 mV. (C) The summary of drug effects normalized to baseline. (D) The representative tracings of I_{Na} obtained by a pulse protocol shown in the inset before apamin (a), after apamin (b) at time points indicated by arrows a and b, respectively, in (E). (E) The time course of peak I_{Na} at −40 mV. (F) The summary of current densities before and after apamin.
doi:10.1371/journal.pone.0096691.g007

be present in cardiac tissues and play an important role in atrial repolarization [5–12]. Apamin also prolongs the action potential duration in diseased ventricles, such as in heart failure, myocardial infarction and after atrioventricular block [14–16,18,19]. However, because previous studies showed that apamin inhibited L-type Ca^{2+} currents [20–22] and Na^+ currents [23] in fetal heart tissue, it is possible that apamin also has non-specific effects on ion channels in adult cardiac tissues. If this is the case, the validity of all research using apamin as a SK inhibitor to explore the role of SK in the heart would in question. For example, if apamin can inhibit any one of the major repolarization currents, such as I_{Ks} or I_{Kr}, then the prolongation of action potential duration after apamin demonstrated in all optical mapping or patch clamp studies may be a result of inhibition of those major ionic currents, and not exclusively from the inhibition of SK currents [15,36,37]. If apamin inhibits I_{to}, then the observed effect of apamin in atria may be explained by I_{to} inhibition since that current is abundantly present in the atria [38–41]. If apamin could affect I_{K1}, then the change of arrhythmia burden after apamin administration could in part come from resting membrane potential shift due to I_{K1} inhibition [17,42,43]. If apamin could affect I_{Na}, then apamin would affect propagation velocity and excitability of heart tissue and thereby influence the arrhythmogenesis. In addition, if apamin inhibits I_{CaL}, then the latter effect may explain the flattening of action potential duration restitution curve in failing ventricles by apamin [15]. Therefore, if apamin is a nonspecific ion channel blocker, the effects of apamin on arrhythmogenesis may not come from SK channel inhibition alone. Because an extensive literature search showed no other studies that have tested the specificity of apamin in human cardiac ion channels, our study is both novel and important for interpreting the antiarrhythmic and proarrhythmic mechanisms of SK current inhibition evaluated using apamin.

In the present study, we used HEK 293 cell line and isolated rabbit ventricular myocytes to study apamin specificity. The HEK 293 cell line was originally derived from human embryonic kidney cells and has the advantage of high transfectability and being easy to culture. This cell line has relatively small endogenous currents compared to the currents expressed in transfected cells (Figure 1), making contamination by endogenous currents insignificant. HEK 293 cells have been widely used to express cloned cardiac ion channels, including Nav1.5 [44,45], Cav1.2 [46–48], Kv7.1 [49], Kv11.1 [31,50], Kir2.1 [51] and Kv4.3 [52] channels. The currents exhibited in the present experiments are consistent with those reports. The concentration of apamin tested most commonly in this study was 500 nM, which is more than 1000 times the reported IC_{50} (0.027~0.095 nM) of the SK2 currents in HEK 293 cells [53–55]. Five hundred nM is also higher than the dose used to block Ca^{2+} and Na^+ currents in chick embryo reaggregates by Bkaily et al [20,21,23]. In addition to HEK 293 cells, we also performed studies in isolated rabbit ventricular myocytes and showed that apamin failed to block either I_{Na} or I_{CaL}. The differences between our results and those reported by Bkaily et al. might have come from species differences or the differences of isoforms between adult and fetal ion channels.

Limitations of the study. Because we did not test the fetal isoform-encoded ionic currents or ionic currents of various possible splicing isoforms in all animal species, our results are only applicable to the most common isoforms of adult human cardiac cells. It is also possible that in native cardiac myocytes, some of these channels have different subunit combinations that we did not test, or their regulation may be different. In the intact heart, ionic currents are also affected by autonomic nerves sensitive to apamin. Since cell environments of HEK cells and rabbit cardiomyocytes are very different from human cardiomyocytes, there is a possibility that apamin may show some effects on the ion channels that we studied in human cardiomyocytes. Further studies using human cells will be warranted.

Conclusions

We conclude that apamin does not have significant effects on the most common isoforms underlying the major human cardiac ion channels. These findings support prior evidence that apamin is a highly selective inhibitor of SK current in the cardiomyocytes.

Supporting Information

Figure S1 A representative time course of I_{Ca} in transfected HEK 293 cells measured at 0 mV. Apamin and nifedipine was added during rundown.
(TIF)

Acknowledgments

We thank Dr. Carol Vandenberg for providing KCNJ2/pCMS-EGFP plasmids, Dr. Minoru Horie for providing KCNH2 and KCNE2 plasmids and Dr. Charles Antzelevitch for providing CACNA1c andCACNB2b plasmids. We thank Nicole Courtney, Jessica Warfel and Jian Tan for their technical assistance.

Author Contributions

Conceived and designed the experiments: CCY TA PSC. Performed the experiments: CCY. Analyzed the data: CCY TA. Contributed reagents/materials/analysis tools: TA PSC. Wrote the paper: CCY TA JW PSC.

References

1. Allen D, Bond CT, Lujan R, Ballesteros-Merino C, Lin MT, et al. (2011) The SK2-long isoform directs synaptic localization and function of SK2-containing channels. Nat Neurosci 14: 744–749.
2. Kohler M, Hirschberg B, Bond CT, Kinzie JM, Marrion NV, et al. (1996) Small-conductance, calcium-activated potassium channels from mammalian brain. Science 273: 1709–1714.
3. Castle NA, Haylett DG, Jenkinson DH (1989) Toxins in the characterization of potassium channels. Trends Neurosci 12: 59–65.
4. Ishii TM, Maylie J, Adelman JP (1997) Determinants of apamin and d-tubocurarine block in SK potassium channels. J Biol Chem 272: 23195–23200.
5. Xu Y, Tuteja D, Zhang Z, Xu D, Zhang Y, et al. (2003) Molecular identification and functional roles of a Ca^{2+}-activated K^+ channel in human and mouse hearts. J Biol Chem 278: 49085–49094.
6. Nie L, Song H, Chen MF, Chiamvimonvat N, Beisel KW, et al. (2004) Cloning and expression of a small-conductance Ca^{2+}-activated K^+ channel from the mouse cochlea: coexpression with alpha9/alpha10 acetylcholine receptors. J Neurophysiol 91: 1536–1544.
7. Tuteja D, Xu D, Timofeyev V, Lu L, Sharma D, et al. (2005) Differential expression of small-conductance Ca^{2+}-activated K^+ channels SK1, SK2, and SK3 in mouse atrial and ventricular myocytes. Am J Physiol Heart Circ Physiol 289: H2714–2723.
8. Lu L, Zhang Q, Timofeyev V, Zhang Z, Young JN, et al. (2007) Molecular coupling of a Ca^{2+}-activated K^+ channel to L-type Ca^{2+} channels via alpha-actinin2. Circ Res 100: 112–120.
9. Zhang Q, Timofeyev V, Lu L, Li N, Singapuri A, et al. (2008) Functional roles of a Ca^{2+}-activated K^+ channel in atrioventricular nodes. Circ Res 102: 465–471.
10. Li N, Timofeyev V, Tuteja D, Xu D, Lu L, et al. (2009) Ablation of a Ca^{2+}-activated K^+ channel (SK2 channel) results in action potential prolongation in atrial myocytes and atrial fibrillation. J Physiol 587: 1087–1100.
11. Lu L, Timofeyev V, Li N, Rafizadeh S, Singapuri A, et al. (2009) Alpha-actinin2 cytoskeletal protein is required for the functional membrane localization of a Ca^{2+}-activated K^+ channel (SK2 channel). Proc Natl Acad Sci U S A 106: 18402–18407.
12. Tuteja D, Rafizadeh S, Timofeyev V, Wang S, Zhang Z, et al. (2010) Cardiac small conductance Ca^{2+}-activated K^+ channel subunits form heteromultimers via the coiled-coil domains in the C termini of the channels. Circ Res 107: 851–859.

13. Nagy N, Szuts V, Horvath Z, Seprenyi G, Farkas AS, et al. (2009) Does small-conductance calcium-activated potassium channel contribute to cardiac repolarization? J Mol Cell Cardiol 47: 656–663.
14. Chang PC, Hsieh YC, Hsueh CH, Weiss JN, Lin SF, et al. (2013) Apamin Induces Early Afterdepolarizations and Torsades de Pointes Ventricular Arrhythmia From Failing Rabbit Ventricles Exhibiting Secondary Rises in Intracellular Calcium. Heart Rhythm 10: 1516–1524.
15. Hsieh YC, Chang PC, Hsueh CH, Lee YS, Shen C, et al. (2013) Apamin-sensitive potassium current modulates action potential duration restitution and arrhythmogenesis of failing rabbit ventricles. Circ Arrhythm Electrophysiol 6: 410–418.
16. Lee YS, Chang PC, Hsueh CH, Maruyama M, Park HW, et al. (2013) Apamin-Sensitive Calcium-Activated Potassium Currents in Rabbit Ventricles with Chronic Myocardial Infarction. J Cardiovasc Electrophysiol 24: 1144–1153.
17. Gui L, Bao Z, Jia Y, Qin X, Cheng ZJ, et al. (2013) Ventricular tachyarrhythmias in rats with acute myocardial infarction involves activation of small-conductance Ca^{2+}-activated K^+ channels. Am J Physiol Heart Circ Physiol 304: H118–130.
18. Chua SK, Chang PC, Maruyama M, Turker I, Shinohara T, et al. (2011) Small-Conductance Calcium-Activated Potassium Channel and Recurrent Ventricular Fibrillation in Failing Rabbit Ventricles. Circ Res 108: 971–979.
19. Chang P-C, Turker I, Lopshire JC, Masroor S, Nguyen BL, et al. (2013) Heterogeneous upregulation of apamin-sensitive potassium currents in failing human ventricles. JAHA 1: e004713.
20. Bkaily G, Sperelakis N, Renaud JF, Payet MD (1985) Apamin, a highly specific Ca^{2+} blocking agent in heart muscle. Am J Physiol 248: H961–965.
21. Bkaily G, Sculptoreanu A, Jacques D, Economos D, Menard D (1992) Apamin, a highly potent fetal L-type Ca^{2+} current blocker in single heart cells. Am J Physiol 262: H463–471.
22. Schetz JA, Anderson PA (1995) Pharmacology of the high-affinity apamin receptor in rabbit heart. Cardiovasc Res 30: 755–762.
23. Bkaily G, Jacques D, Sculptoreanu A, Yamamoto T, Carrier D, et al. (1991) Apamin, a highly potent blocker of the TTX- and Mn^{2+}-insensitive fast transient Na+ current in young embryonic heart. J Mol Cell Cardiol 23: 25–39.
24. Ishikawa T, Sato A, Marcou CA, Tester DJ, Ackerman MJ, et al. (2012) A novel disease gene for Brugada syndrome: sarcolemmal membrane-associated protein gene mutations impair intracellular trafficking of hNav1.5. Circ Arrhythm Electrophysiol 5: 1098–1107.
25. Turker I, Yu CC, Chang PC, Chen Z, Sohma Y, et al. (2013) Amiodarone inhibits apamin-sensitive potassium currents. PLoS One 8: e70450.
26. Aoike F, Takahashi MP, Sakoda S (2006) Class Ic antiarrhythmics block human skeletal muscle Na channel during myotonia-like stimulation. Eur J Pharmacol 532: 24–31.
27. Veselovskii NS, Fedulova SA (1986) [Effect of replacing calcium ions with barium ions in studies of the inward currents of mammalian neurons]. Neirofiziologiia 18: 313–318.
28. Antzelevitch C, Pollevick GD, Cordeiro JM, Casis O, Sanguinetti MC, et al. (2007) Loss-of-function mutations in the cardiac calcium channel underlie a new clinical entity characterized by ST-segment elevation, short QT intervals, and sudden cardiac death. Circulation 115: 442–449.
29. Ai T, Horie M, Obayashi K, Sasayama S (1998) Accentuated antagonism by angiotensin II on guinea-pig cardiac L-type Ca-currents enhanced by beta-adrenergic stimulation. Pflugers Arch 436: 168–174.
30. Yamashita F, Horie M, Kubota T, Yoshida H, Yumoto Y, et al. (2001) Characterization and subcellular localization of KCNQ1 with a heterozygous mutation in the C terminus. J Mol Cell Cardiol 33: 197–207.
31. Zhou Z, Gong Q, Ye B, Fan Z, Makielski JC, et al. (1998) Properties of HERG channels stably expressed in HEK 293 cells studied at physiological temperature. Biophys J 74: 230–241.
32. Abrams CJ, Davies NW, Shelton PA, Stanfield PR (1996) The role of a single aspartate residue in ionic selectivity and block of a murine inward rectifier K^+ channel Kir2.1. J Physiol 493 (Pt 3): 643–649.
33. Faivre JF, Calmels TP, Rouanet S, Javre JL, Cheval B, et al. (1999) Characterisation of Kv4.3 in HEK293 cells: comparison with the rat ventricular transient outward potassium current. Cardiovasc Res 41: 188–199.
34. Habermann E (1984) Apamin. Pharmacol Ther 25: 255–270.
35. Adelman JP, Maylie J, Sah P (2012) Small-Conductance Ca^{2+}-Activated K^+ Channels: Form and Function. Annu Rev Physiol 74: 245–269.
36. Koumi S, Sato R, Hayakawa H (1994) Modulation of the delayed rectifier K^+ current by apamin in guinea-pig heart. Eur J Pharmacol 261: 213–216.
37. Lee YS, Chang PC, Hsueh CH, Maruyama M, Park HW, et al. (2013) Apamin-Sensitive Calcium-Activated Potassium Currents in Rabbit Ventricles with Chronic Myocardial Infarction. J Cardiovasc Electrophysiol.
38. Sosunov EA, Anyukhovsky EP, Hefer D, Rosen TS, Danilo P Jr, et al. (2005) Region-specific, pacing-induced changes in repolarization in rabbit atrium: an example of sensitivity to the rare. Cardiovasc Res 67: 274–282.
39. Ozgen N, Dun W, Sosunov EA, Anyukhovsky EP, Hirose M, et al. (2007) Early electrical remodeling in rabbit pulmonary vein results from trafficking of intracellular SK2 channels to membrane sites. Cardiovasc Res 75: 758–769.
40. Hsueh CH, Chang PC, Hsieh YC, Reher T, Chen PS, et al. (2013) Proarrhythmic effect of blocking the small conductance calcium activated potassium channel in isolated canine left atrium. Heart Rhythm 10: 891–898.
41. Chen WT, Chen YC, Lu YY, Kao YH, Huang JH, et al. (2013) Apamin modulates electrophysiological characteristics of the pulmonary vein and the Sinoatrial Node. Eur J Clin Invest 43: 957–963.
42. Chang PC, Hsieh YC, Hsueh CH, Weiss JN, Lin SF, et al. (2013) Apamin induces early afterdepolarizations and torsades de pointes ventricular arrhythmia from failing rabbit ventricles exhibiting secondary rises in intracellular calcium. Heart Rhythm.
43. Chua SK, Chang PC, Maruyama M, Turker I, Shinohara T, et al. (2011) Small-conductance calcium-activated potassium channel and recurrent ventricular fibrillation in failing rabbit ventricles. Circ Res 108: 971–979.
44. Shuraih M, Ai T, Vatta M, Sohma Y, Merkle EM, et al. (2007) A common SCN5A variant alters the responsiveness of human sodium channels to class I antiarrhythmic agents. J Cardiovasc Electrophysiol 18: 434–440.
45. Wu G, Ai T, Kim JJ, Mohapatra B, Xi Y, et al. (2008) alpha-1-syntrophin mutation and the long-QT syndrome: a disease of sodium channel disruption. Circ Arrhythm Electrophysiol 1: 193–201.
46. Templin C, Ghadri JR, Rougier JS, Baumer A, Kaplan V, et al. (2011) Identification of a novel loss-of-function calcium channel gene mutation in short QT syndrome (SQTS6). Eur Heart J 32: 1077–1088.
47. Dalton S, Takahashi SX, Miriyala J, Colecraft HM (2005) A single CaVbeta can reconstitute both trafficking and macroscopic conductance of voltage-dependent calcium channels. J Physiol 567: 757–769.
48. Kamp TJ, Hu H, Marban E (2000) Voltage-dependent facilitation of cardiac L-type Ca channels expressed in HEK-293 cells requires beta-subunit. Am J Physiol Heart Circ Physiol 278: H126–136.
49. Dong MQ, Sun HY, Tang Q, Tse HF, Lau CP, et al. (2010) Regulation of human cardiac KCNQ1/KCNE1 channel by epidermal growth factor receptor kinase. Biochim Biophys Acta 1798: 995–1001.
50. Sakaguchi T, Itoh H, Ding WG, Tsuji K, Nagaoka I, et al. (2008) Hydroxyzine, a first generation H(1)-receptor antagonist, inhibits human ether-a-go-go-related gene (HERG) current and causes syncope in a patient with the HERG mutation. J Pharmacol Sci 108: 462–471.
51. Ballester LY, Benson DW, Wong B, Law IH, Mathews KD, et al. (2006) Trafficking-competent and trafficking-defective KCNJ2 mutations in Andersen syndrome. Hum Mutat 27: 388.
52. Giudicessi JR, Ye D, Tester DJ, Crotti L, Mugione A, et al. (2011) Transient outward current (I(to)) gain-of-function mutations in the KCND3-encoded Kv4.3 potassium channel and Brugada syndrome. Heart Rhythm 8: 1024–1032.
53. Benton DC, Monaghan AS, Hosseini R, Bahia PK, Haylett DG, et al. (2003) Small conductance Ca^{2+}-activated K^+ channels formed by the expression of rat SK1 and SK2 genes in HEK 293 cells. J Physiol 553: 13–19.
54. Grunnet M, Jensen BS, Olesen SP, Klaerke DA (2001) Apamin interacts with all subtypes of cloned small-conductance Ca^{2+}-activated K^+ channels. Pflugers Arch 441: 544–550.
55. Strobaek D, Jorgensen TD, Christophersen P, Ahring PK, Olesen SP (2000) Pharmacological characterization of small-conductance Ca^{2+}-activated K^+ channels stably expressed in HEK 293 cells. Br J Pharmacol 129: 991–999.